Key Engineering Materials
ISSN: 1662-9795, Vol. 1049, pp 55-63
doi:10.4028/p-Nz9UGU

Submitted: 2026-01-16
Revised: 2026-02-13
Accepted: 2026-02-24
Online: 2026-04-15

Uncertainty Detection in Sheet Metal Bending Processes with Machine Learning

Tomás Parreira[1,a *], Daniel Cruz[2,b], Armando Marques[1,c], Pedro Prates[1,3,d], Marta Oliveira[1,e], Abel Santos[2,f], Bernardete Ribeiro[4,g] and André Pereira[1,h]

[1]Centre for Mechanical Engineering, Materials and Processes (CEMMPRE), University of Coimbra, Portugal.

[2]Institute of Science and Innovation in Mechanical and Industrial Engineering Department (INEGI), Porto, Portugal

[3]List Centre for Mechanical Technology and Automation (TEMA), University of Aveiro, Portugal

[4]Centre for Informatics and Systems of the University of Coimbra (CISUC), Informatics Department, University of Coimbra, Portugal

[a]tomas.parreira@dem.uc.pt (*corresponding author), [b]dcruz@inegi.up.pt, [c]armando.marques@uc.pt, [d]prates@ua.pt, [e]marta.oliveira@dem.uc.pt, [f]abel@fe.up.pt, [g]bribeiro@dei.uc.pt, [h]andre.pereira@uc.pt

Keywords: Uncertainty Detection, Machine Learning, Forming Processes, Bending Processes

Abstract. The quality and dimensional accuracy of sheet metal components are strongly influenced by various sources of uncertainty, including variations in material properties, tool geometry and process parameters. Determining the specific source responsible for deviations in bending outcomes is usually costly and time-consuming, especially in industrial settings where numerous factors interact. In this study, a machine learning framework that can detect and quantify the impact of uncertainties in both air and bottom bending processes is presented. A dataset comprising forming results such as bending angles, final thickness and measured deviations, is used to train two neural network metamodels (one for each process) that link input uncertainties to process outcomes. The predictive performance of these models was evaluated using different metrics achieving high predictive accuracy, with coefficients of determination close to 1 for most uncertainty sources in air bending and values above 0.95 for the majority of parameters in bottom bending. These results demonstrate the capability of the methodology to reliably identify dominant sources of uncertainty and support robust process optimization.

Introduction

In sheet metal forming, the central challenge is ensuring that a part can be formed reliably across repeated production cycles. Experience in the industry shows that parts which are nominally identical in terms of geometry, tooling and process parameters can still exhibit significant variation in terms of final shape, thickness distribution and failure location [1,2]. This variability is an intrinsic characteristic of forming operations driven by unavoidable fluctuations in material properties, surface conditions, tool wear and machine behaviour. Consequently, predictive models that aim solely for nominal accuracy often prove inadequate when moved from controlled environments to real manufacturing systems [3]. From this perspective, it's required to understand how sensitive a process is to perturbations, which parameters dominate variability and how robust a given tool or process design is under realistic operating conditions [4]. This requirement is particularly important in sheet metal forming, where plastic instability, elastic recovery and contact-driven effects coexist [5].

Finite element analysis (FEA) remains an indispensable tool as it provides detailed insights into stress and strain evolution. However, FEA is computationally demanding [6] and ignores the role of uncertainty and its influence on the forming results. Consequently, decisions driven by FEA often rely on limited scenarios, implicitly assuming that unmodelled variability is negligible, an assumption that can be costly in production environments [7]. In this context, uncertainty quantification (UQ) emerged as a key tool, enabling input variability to be propagated through numerical models and

output dispersion to be quantified. Rather than providing deterministic forming results, UQ-based analyses deliver probabilistic results and sensitivity rankings [8]. This enables engineers to assess risk, compare alternative designs, and identify which parameters should be more accurately characterized and controlled.

However, the application of UQ-based analyses is generally associated with a high computational cost, which limits their applicability. This has motivated the development of data-driven surrogate models [9,10]. Machine learning models trained on numerical or hybrid numerical–experimental datasets have demonstrated an ability to approximate complex forming outcomes at a negligible evaluation cost [11,12]. These models facilitate more extensive parameter studies, real-time prediction, and integration with optimization or control frameworks [13], while also making detailed physical simulations more accessible in industrial practice, even for operators without specialized expertise [14]. Furthermore, the speed and accessibility of surrogate models enable their integration with in-process data, allowing real-time updates of process states and adaptive control strategies [15,16]. Despite these advances, significant challenges remain. Surrogate models must generalize reliably beyond the conditions encountered during training; uncertainty analyses must be feasible for industrial-scale problems; and the trade-off between model accuracy and decision quality must be carefully managed [17]. Addressing these challenges requires integrated methodologies that treat variability as a primary modelling objective rather than a secondary concern.

The present work explores the use of Machine Learning to detect the uncertainty factors causing deviations in the final formed part. The goal is to establish a relationship between the forming results and the uncertainty factors. This will enable the introduction of forming results into the machine learning model to predict the source of defects in the final part and identify those that are out of an acceptable range. The proposed strategy is demonstrated for the air and bottom bending processes. Initially, a numerical database was generated, consisting of forming results obtained from numerical simulations under varying uncertainty sources associated with tools parameters. Next, two neural network algorithms were trained to link each uncertainty to the forming results of the bending processes. The approach was validated using unseen data, and its performance was evaluated using different metrics.

Numerical Model

The numerical model of this forming process consists of two tools, the punch and the die, whose relevant parameters are identified in Fig. 1 and will be further explored in detail.

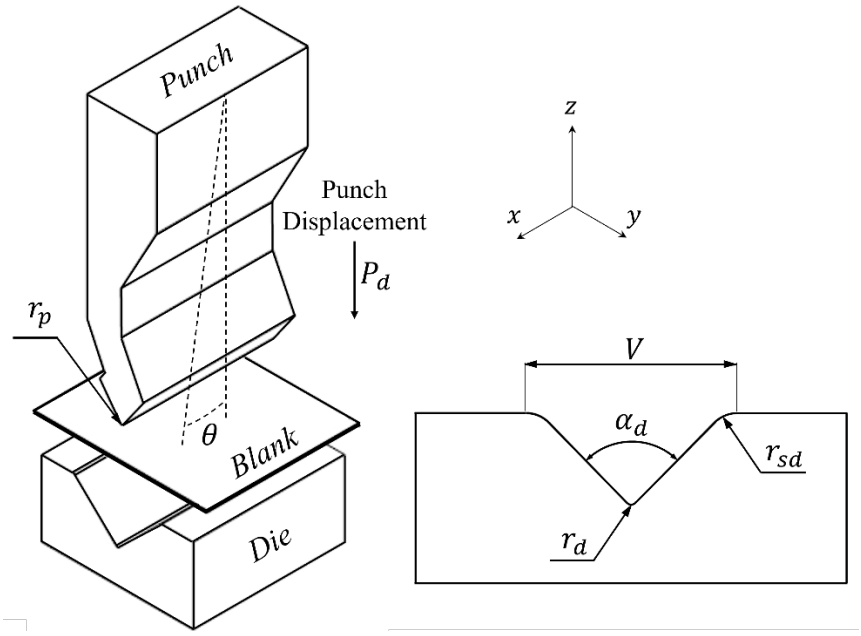

Fig. 1. Parameters considered in the bending processes.

For this work, a dual phase steel "DP600" was considered. The plastic behaviour is described by the Hill'48 orthotropic yield criterion [18] and the Swift hardening law [19]. The Hill'48 orthotropic yield criterion is defined as follows:

$$F(\sigma_{yy}-\sigma_{zz})^2+G(\sigma_{zz}-\sigma_{xx})^2+H(\sigma_{xx}-\sigma_{yy})^2+2L\tau_{yz}^2+2M\tau_{xz}^2+2N\tau_{xy}^2=Y^2, \quad (1)$$

where Y is the yield stress, F, G, H, L, M and N are the parameters that define the shape of the yield surface, and σ_{xx}, σ_{yy}, σ_{zz}, τ_{xy}, τ_{xz} and τ_{yz} are components of the Cauchy stress tensor, written in the orthotropic coordinate system O_{xyz}. In this work, it is assumed that $L=M=1.5$ (identical to von Mises) and $G+H=1$, meaning that the hardening curve, $Y(\bar{\varepsilon}^p)$, is comparable to the uniaxial tensile stress aligned with the rolling direction. The evolution of yield stress with plastic deformation, Y, is described by the Swift hardening law:

$$Y=K\,(\varepsilon_0+\bar{\varepsilon}^p)^n, \quad (2)$$

where K, ε_0 and n are material constants, and $\bar{\varepsilon}^p$ is the equivalent plastic strain. The constitutive parameters of the DP600 material were characterized in [20] and are presented in Table 1.

Table 1. Constitutive parameters of the DP600 material characterized in [20].

F	G	H	N	r_0	r_{45}	r_{90}
0.506	0.59	0.41	1.572	0.695	0.935	0.812
n	Y_0 [MPa]	K [MPa]	E [GPa]	v		
0.1426	430.5	975.73	210	0.3		

The friction between the tools and the blank was assumed to be described by Coulomb's law with a constant friction coefficient, M_u. Contact uses the augmented Lagrangian method. The blank is discretized with 30576 (8-node hexahedral solid) elements, with 6 elements in thickness, combined with a selective reduced integration technique [21]. The tools are modelled as rigid bodies described by Bézier surfaces, with all displacements fully constrained except for the punch, which is allowed to move along the z-axis. The numerical simulations were performed using the software DD3IMP (Deep Drawing 3D Implicit Code), which uses an updated Lagrangian scheme to integrate the constitutive law in an implicit way. Each air bending simulation took an average of 10 minutes and the bottom bending simulation an average of 35 minutes to complete on computers equipped with an Intel® Core™ i7-13900K processor (5.8 GHz).

Uncertainty Model

The numerical simulations of the two processes were conducted by systematically varying the considered parameters (presented in Table 2) following a Sobol sequence [22], allowing a better representation of the input space. The uncertainty parameters (that will be the output of the models and were presented in Fig.1) are the radius of the punch (r_p), the punch displacement (P_d), the punch angular misalignment in relation to the blank (θ), the superior die radius (r_{sd}), the die bottom radius (r_d) and the length of the die (V). For the air bending process the parameter (r_d) is not an output value as the blank does not reach the bottom part of the die. Similarly, for the bottom bending process the punch displacement (P_d) is not an output value as this parameter is fixed, the punch moves until it reaches contact with the bottom part of the die (for the air bending process it is defined as a percentage of the full possible punch displacement). The superior die radius (r_{sd}), is also not considered in the bottom bending as it has very low influence in the final part geometry. In Table 2 the interval of variation of these parameters is presented.

Table 2. Minimum and maximum values for the uncertainty sources.

	r_p [mm]	P_d [%]	θ[°]	r_{sd} [mm]	r_d [mm]	V [mm]
min	0.5	0.45	-0.75	3.5	0.5	24
mean	1.0	0.50	0	4	1.0	25
max	1.5	0.55	0.75	4.5	1	26

Machine Learning Approaches

In this work a machine learning approach is used to detect the uncertainty source based on the forming results of the bending processes. Once the models are constructed (one model per process) it will be possible to predict the uncertainty value based on the deviations of the forming results. The dataset used to train the models was generated by gathering the results of the numerical simulations.

Air Bending

For the air bending process a total of 3000 simulations were performed following the Sobol sequence as described above. The forming results (inputs) considered were the initial thickness of the blank (t_0), the final thickness measured in the exact center of the part (t_f), the die bottom radius (r_d), the inner radius (r_i) and external radius (r_e) of the final part evaluated in both sides. Additionally, the die opening angle (α_d), the final part angle (α_f) (after springback) in both sides of the part were also considered. In Fig. 2 the parameters that depend on the final geometry of the part are presented. A total of 32 force values, uniformly distributed along the punch displacement up to the maximum simulated displacement, were considered. In total, the dataset consisted of 42 inputs and 5 outputs (the punch angular misalignment in relation to the blank (θ), punch radius (r_p), the punch displacement (P_d), the superior die radius (r_{sd}) and the length of the die (V)).

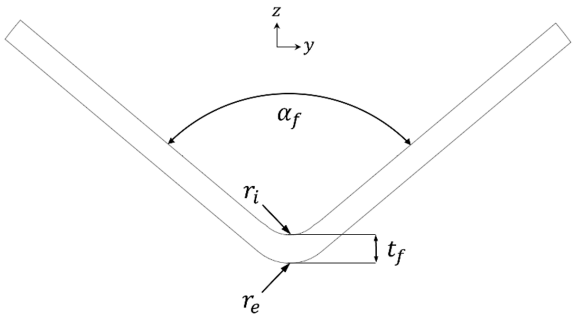

Fig. 2. Geometry parameters considered in the dataset.

A multi-output deep neural network was developed using *TensorFlow/Keras* to predict multiple process parameters simultaneously. The dataset was split into training and testing subsets with an 85/15 ratio, and all features and targets were standardized using *StandardScaler* to improve convergence during training. The network architecture consists of an input block with 512 units and a hyperbolic tangent (*tanh*) activation function. The hidden block includes three main fully connected layers with 512, 128, and 256 neurons, respectively, each using the *Scaled Exponential Linear Unit* (*SELU*) activation. Each target variable is predicted through an independent linear output head, enabling multi-output regression with separate loss functions. The model was optimized using the *Adam* algorithm with a learning rate of 7.01×10^{-5}. The network was trained for 2000 epochs and the hyperparameters were selected through a randomized search over multiple configurations, including variations in layer sizes, activation functions, dropout rates, and optimizer choices. Early stopping and learning rate reduction were employed during this search to prevent overfitting and improve convergence.

Bottom Bending

For the bottom bending process, a total of 2025 simulations were carried out. The database consisted of the initial thickness of the blank (t_0), the final thickness measured in the exact center of the final part (t_f), a total of 38 force values (measured in intervals of 0.3 mm of punch displacement, the maximum displacement was 11.4 mm), the inner (r_i) and external (r_e) radius of the final part for both sides. Additionally, the die angle (α_d) and the final part angle (α_f) (after springback) on both sides of the part were considered. In total, the dataset comprised 48 inputs and 4 outputs (the punch angular misalignment in relation to the blank (θ), punch radius (r_p), the die bottom radius (r_d) and the length of the die (V)).

A second multi-output deep neural network was developed using *TensorFlow/Keras* to predict the four mentioned output parameters. As in the previous model, the data were split into training and testing subsets with an 85/15 ratio and features and targets were standardized using *StandardScaler*. The network architecture is similar to the previous model, consisting of an input block followed by multiple hidden layers and a final output block. The input layer contains 1536 units with a hyperbolic tangent (*tanh*) activation function. Three hidden layers were included with 512, 512, and 128 neurons, respectively, using *SELU* activation. The key difference lies in the output layer. This network uses a single output layer with four neurons, each neuron predicting one of the target variables simultaneously. This approach allows simultaneous multi-output regression but applies the loss function globally rather than individually to each target. The network was optimized using the *Nadam* algorithm with a learning rate of approximately 1×10^{-4}, and mean squared error (MSE) was used as the loss function with mean absolute error (MAE) as an evaluation metric. Training was conducted for 2000 epochs and hyperparameters were selected through a randomized search, similarly to the previous model, exploring variations in layer sizes, activation functions, dropout rates, and optimizer choice. While both models address a multi-output regression problem, the first adopts a multi-head architecture with independent output layers and losses for each target, whereas the second employs a single shared output layer, jointly optimizing all target variables within a unified loss function. This choice was made to explore potential differences in the predictive performance of the two architectures, and to investigate whether modelling the outputs independently or jointly better captures the relationships among the target variables.

Results

This section presents the results of the predictions of the uncertainty sources values based on the forming results of the bending processes. After the simulations, the forming results were input into the trained models to assess their predictive performance. Fig. 3 (air bending) and Fig.4 (bottom bending) show a comparison between the real and predicted values of the uncertainty source based on the forming results from the test set (15% of the total number of simulations). To quantify the predictive performance of the models the Mean Absolute Error (MAE), Root Mean Squared Error (RMSE), and the coefficient of determination (R^2) were calculated for each parameter. It can be concluded that in the air bending process three parameters (punch angular misalignment, punch displacement and die length) show a very high coefficient of determination, almost 1, as the model can predict the real value of the parameter in almost every test sample. For the punch and superior die radius the coefficient of determination is lower, around 0.95, but still at a high value, showing great accuracy overall. For the bottom bending process, the results show an inferior performance as the die length parameter gets down to a coefficient of determination of 0.92. The other parameters still show results above 0.95 and therefore a good prediction performance overall. The MAE and RMSE metrics follow the same tendency as the R^2.

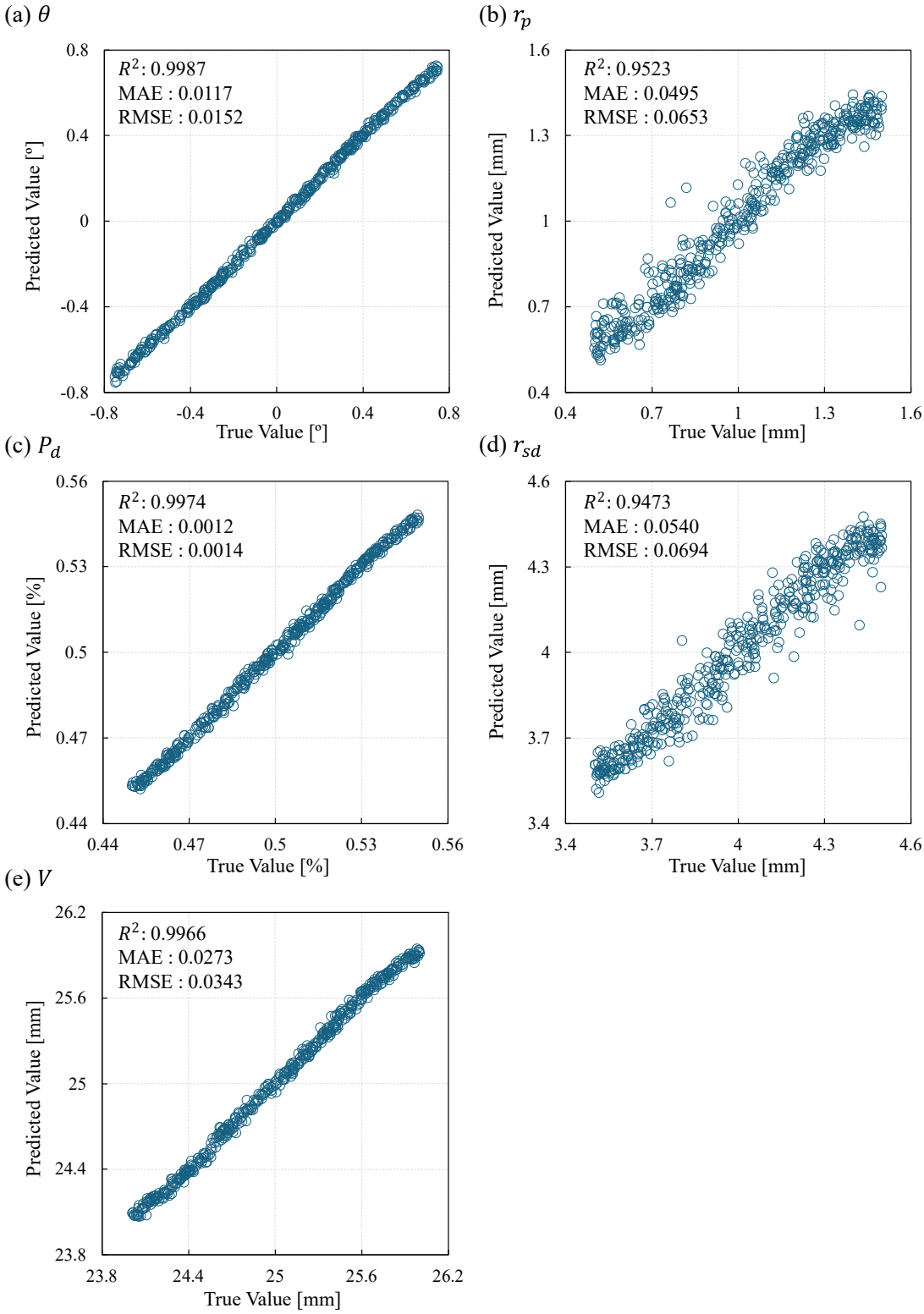

Fig. 3. Predicted and real values for the uncertainty sources in air bending: (a) θ; (b) r_p; (c) P_d; (d) r_{sd}; (e) V.

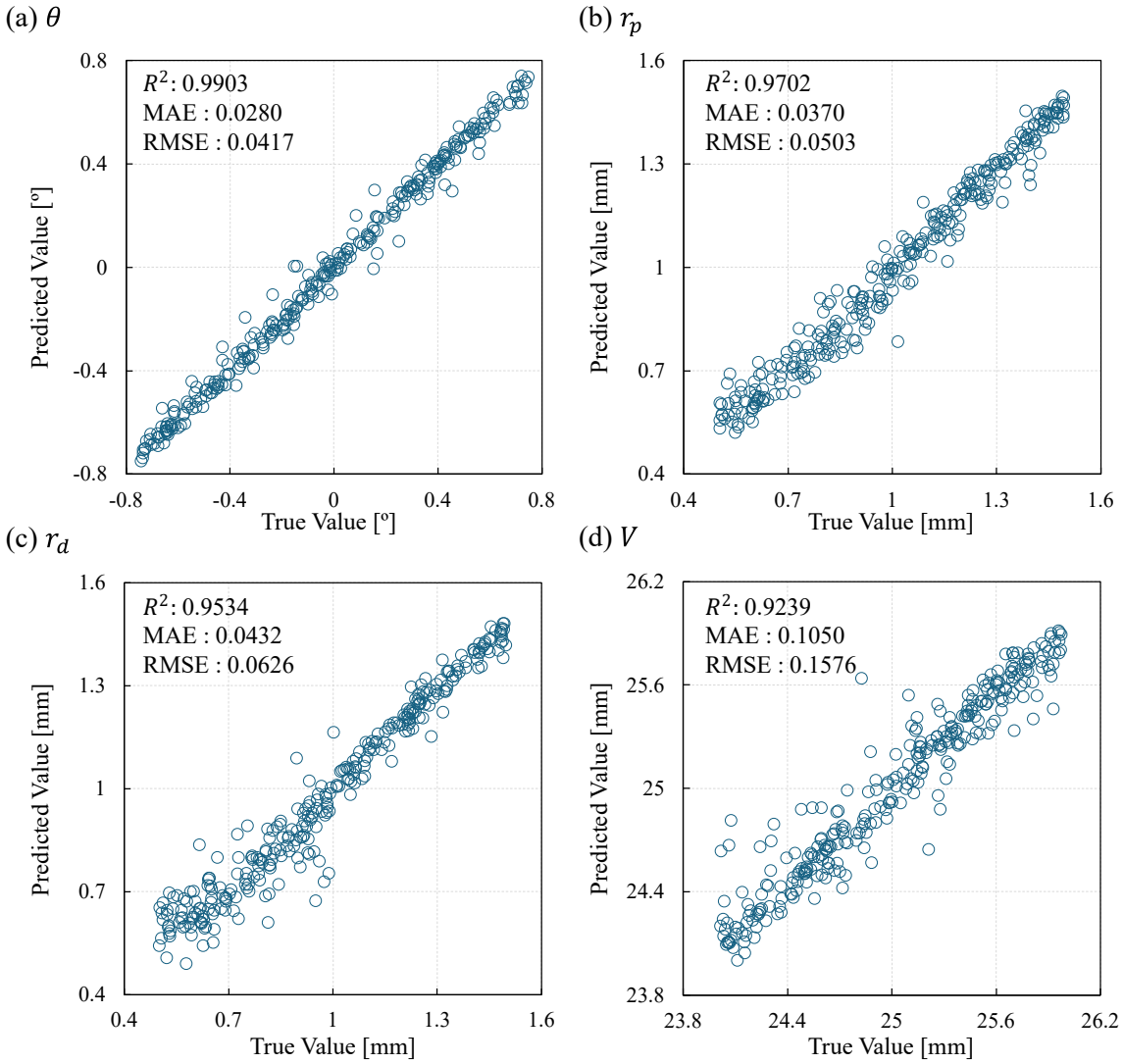

Fig. 4. Predicted and real values for the uncertainty sources in bottom bending: (a) θ; (b) r_p; (c) r_d; (d) V.

Conclusions

This work proposes a methodology to identify the sources of uncertainty responsible for possible deviations in the forming results of the final part both in the air bending and the bottom bending process, namely radius of the punch (r_p), the punch displacement (P_d), the punch angular misalignment in relation to the blank (θ), the superior die radius (r_{sd}), the die bottom radius (r_d) and the length of the die (V). It uses machine learning to build models (one per process) to establish relationships between the forming results and the uncertainty sources. Artificial Neural Networks were constructed based on a dataset consisting of numerical results from the bending processes and the values of the uncertainties in that simulation. The performance of the models was evaluated, and the hyperparameters were defined to achieve maximum model performance. For both processes, all predicted outputs reached a coefficient of determination (R^2) over 0.9 with parameters such as the punch angular misalignment reaching a score near 1. This work addresses the limitations of surrogate models in bending processes by linking uncertainties in the process and tool geometry to defects in the final part. This provides accurate predictions to support process optimization and robustness control in industrial applications. Future studies will explore alternative modelling strategies, such as different model types or a classification-based framework, and the methodology will undergo experimental validation.

Acknowledgments

This work is sponsored by national funds through FCT – Fundação para a Ciência e a Tecnologia, under the project UID/00285-Centre for Mechanical Engineering, Materials and Processes and LA/P/0112/2020. It was also supported by the projects RealForm (ref. 2022.02370.PTDC), SmartBending (ref. 2023.14606.PEX), LSD-TRIP (ref. COMPETE2030-FEDER-00778700) and A3Shell (ref. COMPETE2030-FEDER-02233400) The author Tomás Parreira was supported by doctoral grant from FCT (2024.00961.BD). All support is gratefully acknowledged.

References

[1] de Souza, T.; Rolfe, B. Multivariate Modelling of Variability in Sheet Metal Forming. *J Mater Process Technol* 2008, *203*, 1–12, doi:10.1016/j.jmatprotec.2007.09.075.

[2] Trzepieciński, T. Recent Developments and Trends in Sheet Metal Forming. *Metals (Basel)* 2020, *10*, 779, doi:10.3390/met10060779.

[3] Liewald, M.; Bergs, T.; Groche, P.; Behrens, B.-A.; Briesenick, D.; Müller, M.; Niemietz, P.; Kubik, C.; Müller, F. Perspectives on Data-Driven Models and Its Potentials in Metal Forming and Blanking Technologies. *Production Engineering* 2022, *16*, 607–625, doi:10.1007/s11740-022-01115-0.

[4] Xie, Y.; Feng, K.; Du, M.; Wang, Y.; Li, L. Robust Optimization of Stamping Process Based on Bayesian Estimation. *J Manuf Process* 2023, *101*, 245–258, doi:10.1016/j.jmapro.2023.06.009.

[5] Hou, Y.; Myung, D.; Park, J.K.; Min, J.; Lee, H.-R.; El-Aty, A.A.; Lee, M.-G. A Review of Characterization and Modelling Approaches for Sheet Metal Forming of Lightweight Metallic Materials. *Materials* 2023, *16*, 836, doi:10.3390/ma16020836.

[6] Folle, L.F.; Lima, T.N.; Santos, M.P.S.; Callegari, B.; Silva, B.C. dos S.; Zamorano, L.G.S.; Coelho, R.S. A Review on Sheet Metal Forming Behavior in High-Strength Steels and the Use of Numerical Simulations. *Metals (Basel)* 2024, *14*, 1428, doi:10.3390/met14121428.

[7] Volodina, V.; Challenor, P. The Importance of Uncertainty Quantification in Model Reproducibility. *Philosophical Transactions of the Royal Society A: Mathematical, Physical and Engineering Sciences* 2021, *379*, rsta.2020.0071, doi:10.1098/rsta.2020.0071.

[8] Prates, P.A.; Adaixo, A.S.; Oliveira, M.C.; Fernandes, J. V. Numerical Study on the Effect of Mechanical Properties Variability in Sheet Metal Forming Processes. *The International Journal of Advanced Manufacturing Technology* 2018, *96*, 561–580, doi:10.1007/s00170-018-1604-y.

[9] Abio, A.; Bonada, F.; Pujante, J.; Grané, M.; Nievas, N.; Lange, D.; Pujol, O. Machine Learning-Based Surrogate Model for Press Hardening Process of 22MnB5 Sheet Steel Simulation in Industry 4.0. *Materials* 2022, *15*, 3647, doi:10.3390/ma15103647.

[10] Hoffer, J.G.; Geiger, B.C.; Kern, R. Gaussian Process Surrogates for Modeling Uncertainties in a Use Case of Forging Superalloys. *Applied Sciences* 2022, *12*, 1089, doi:10.3390/app12031089.

[11] Heinzelmann, P.; Baum, S.; Riedmüller, K.R.; Liewald, M.; Weyrich, M. A Comprehensive Benchmark Dataset for Sheet Metal Forming: Advancing Machine Learning and Surrogate Modelling in Pro-Cess Simulations. *MATEC Web of Conferences* 2025, *408*, 01090, doi:10.1051/matecconf/202540801090.

[12] Han, S.-S.; Kim, H.-K. Artificial Neural Network-Based Sequential Approximate Optimization of Metal Sheet Architecture and Forming Process. *J Comput Des Eng* 2024, *11*, 265–279, doi:10.1093/jcde/qwae049.

[13] Weeks, J.S.; Stebner, A.P. Efficient Multiscale Simulations of Incremental Sheet Forming Using Machine Learning Surrogate Models for Crystal Plasticity. *Integr Mater Manuf Innov* 2025, *14*, 573–592, doi:10.1007/s40192-025-00427-0.

[14] Hürkamp, A.; Gellrich, S.; Dér, A.; Herrmann, C.; Dröder, K.; Thiede, S. Machine Learning and Simulation-Based Surrogate Modeling for Improved Process Chain Operation. *The International Journal of Advanced Manufacturing Technology* 2021, *117*, 2297–2307, doi:10.1007/s00170-021-07084-5.

[15] Link, P.; Penter, L.; Rückert, U.; Klingel, L.; Verl, A.; Ihlenfeldt, S. Real-Time Quality Prediction and Local Adjustment of Friction with Digital Twin in Sheet Metal Forming. *Robot Comput Integr Manuf* 2025, *91*, 102848, doi:10.1016/j.rcim.2024.102848.

[16] Villegas-Ch, W.; Gutierrez, R.; Govea, J. Digital Twin Integration in Metalworking: Enhancing Efficiency and Predictive Maintenance. *Front Mech Eng* 2025, *11*, doi:10.3389/fmech.2025.1655565.

[17] Azarhoosh, Z.; Ilchi Ghazaan, M. A Review of Recent Advances in Surrogate Models for Uncertainty Quantification of High-Dimensional Engineering Applications. *Comput Methods Appl Mech Eng* 2025, *433*, 117508, doi:10.1016/j.cma.2024.117508.

[18] Hill, R. *A Theory of the Yielding and Plastic Flow of Anisotropic Metals*; *Proc. R. Soc. London Ser. A Math. Phys. Sci*. **1948**, 193,281–297.

[19] Swift, H.W. Plastic Instability under Plane Stress. *J Mech Phys Solids* 1952, *1*, 1–18, doi:10.1016/0022-5096(52)90002-1.

[20] Amaral, R. Development of Accurate Numerical Methodologies Applied to the Stamping of Advanced High Strength Steels and Experimental Validation, FACULDADE DE ENGENHARIA DA UNIVERSIDADE DO PORTO, 2020.

[21] Arnst, M.; Ponthot, J.-P.; Boman, R. Comparison of Stochastic and Interval Methods for Uncertainty Quantification of Metal Forming Processes. *Comptes Rendus. Mécanique* 2018, *346*, 634–646, doi:10.1016/j.crme.2018.06.007.

[22] Sobol, I.M. *Sensitivity* Estimates for Nonlinear Mathematical Models. 1993.